A Mixed Incoherent Feed-Forward Loop Allows Conditional Regulation of Response Dynamics

Semsey, Szabolcs

Published in:
P L o S One

DOI:
10.1371/journal.pone.0091243

Publication date:
2014

Document version
Publisher's PDF, also known as Version of record

OPEN ACCESS Freely available online

PLOS ONE

A Mixed Incoherent Feed-Forward Loop Allows Conditional Regulation of Response Dynamics

Szabolcs Semsey*

Center for Models of Life, Niels Bohr Institute, University of Copenhagen, Copenhagen, Denmark

Abstract

Expression of the SodA superoxide dismutase (MnSOD) in Escherichia coli is regulated by superoxide concentration through the SoxRS system and also by Fur (Ferric uptake regulator) through a mixed incoherent feed forward loop (FFL) containing the RyhB small regulatory RNA. In this work I theoretically analyze the function of this feed forward loop as part of the network controlling expression of the two cytoplasmic superoxide dismutases, SodA and SodB. I find that feed forward regulation allows faster response to superoxide stress at low intracellular iron levels compared to iron rich conditions. That is, it can conditionally modulate the response time of a superimposed transcriptional control mechanism.

Citation: Semsey S (2014) A Mixed Incoherent Feed-Forward Loop Allows Conditional Regulation of Response Dynamics. PLoS ONE 9(3): e91243. doi:10.1371/journal.pone.0091243

Editor: Eshel Ben-Jacob, Tel Aviv University, Israel

Received October 19, 2013; **Accepted** February 11, 2014; **Published** March 12, 2014

Funding: This research was supported by the Danish National Research Foundation. The funder had no role in study design, data collection and analysis, decision to publish, or preparation of the manuscript.

Competing Interests: S. Semsey is an Associate Editor at PLOS ONE. This does not alter the author's adherence to all the PLOS ONE policies on sharing data and materials.

* E-mail: semsey@nbi.dk

Introduction

The highly reactive superoxide (O_2^-), which is produced intracellularly as a common byproduct of aerobic life, is one of the main reactive oxygen species that can damage cellular components. Most of the cells exposed to oxygen possess enzymes that provide protection to superoxide toxicity by catalyzing dismutation of superoxide to hydrogen peroxide and oxygen. Extracellular superoxide is produced for instance by phagocytic leukocytes to inactivate invading microorganisms, or by heterotrophic bacteria, affecting global biogeochemistry [1]. Therefore pathogenic bacteria evolved mechanisms to inactivate superoxide molecules or their production in host macrophages [2]. *Escherichia coli* has three superoxide dismutases (SodA, SodB, and SodC) which require different metal cofactors and are regulated in different ways [3–8].

The active SodA, or MnSOD, contains manganese. SodA can bind iron and manganese with similar efficiencies [9] but the iron-substituted SodA is catalytically inactive [10]. SodB, or Fe-SOD, contains iron. The cytosolic SodA and SodB proteins have overlapping functions [11] but they are functionally not equivalent [12]. The periplasmic SodC protein contains copper and zinc, and may be important to protect the cell from macrophage killing [13–15].

Transcription of *sodA*, but not of *sodB*, is activated by superoxide stress through the SoxR-SoxS system [5,16]. Expression of both SodA and SodB is regulated by intracellular iron availability (Figure 1). Transcription of *sodA* is directly inhibited by the iron-bound form of the Ferric Uptake Regulator (Fe-Fur) [8], while *sodB* transcription is independent of Fe-Fur [7]. However, Fe-Fur levels affect SodB protein production through the small regulatory RNA (sRNA) RyhB, which acts by inhibiting translation initiation and by decreasing mRNA stability [17]. SodA expression is also negatively controlled by RyhB [3], therefore SodA expression is inhibited through an incoherent feed-forward loop (FFL). Similar steady-state SodA activities were found in wild type and Δ*fur* strains [8], suggesting that the FFL results in similar levels of repression at both high and low levels of free intracellular iron (Figure 1). In order to pinpoint the function of this FFL, I investigated the performance of feed-forward regulation of SodA compared to a control system where SodA expression is independent of Fe-Fur and RyhB.

Results

I have developed a mathematical model to study the characteristics of feed-forward regulation of SodA expression. The model is described in detail in the *Models* section. Using this model I compared the steady state and dynamic behaviors of the natural system, where SodA expression is regulated by RyhB and Fe-Fur through a FFL, with a hypothetical control where SodA production does not depend on FeFur or RyhB concentration.

The incoherent FFL keeps steady state SodA mRNA levels constant

Similar SodA activities were reported in wild type cells growing in iron rich conditions and in Δ*fur* strains [8] where RyhB is expressed at maximal levels [17]. The parameter values in the model were chosen to match this experimental observation. Thus the model produced similar SodA mRNA levels at high iron (Fe-Fur-repressed) and low iron (RyhB-repressed) conditions.

First I explored the steady-state levels of SodA at intermediate Fe-Fur levels in the absence of superoxide stress. Simulations showed that SodA mRNA levels were kept in a relatively narrow range as Fe-Fur levels were changed from 2 to 2000 nM (Figure 2). Unlike typical regulatory systems which regulate transitions between a high and a low expression state, i.e. turn a gene on

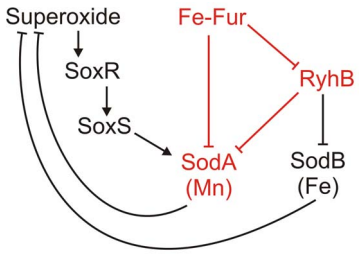

Figure 1. Regulation of cytoplasmic superoxide dismutases by intracellular free iron and superoxide levels. SodA expression is regulated by iron through an incoherent feed-forward loop (shown in red).
doi:10.1371/journal.pone.0091243.g001

or off, this FFL regulates transitions between similar expression states. Although the SodA mRNA has similar concentrations in these states, it has substantially higher turnover (higher production and degradation rates) at low iron levels (Figure 2, dotted line).

Simulations of transitions between low and high iron levels

To explore how SodA mRNA levels respond to changes in iron availability, I simulated sudden changes in Fe-Fur levels (Figure 3). SodA expression responded by a transient increase to iron depletion (~2-fold), and returned to its original level after about 1.5 cell generation (Figure 3A). Such transient expression change, i.e. exhibition of near perfect adaptation, is a typical feature of incoherent FFLs [18–21]. It results from the delay in RyhB mediated inactivation of SodA mRNA, which depend on the rate of RyhB production relative to its targets production rates and on the efficiency of RyhB pairing with the SodA mRNA. To explore how changes in these parameters affect the shape of the response curve, I performed simulations where RyhB was produced at lower rates than the estimated upper bound used in Figure 3A (see *Methods*). To obtain the same steady-state SodA mRNA levels at low and high Fe-Fur levels as with the standard parameters used in Figure 3A, the rate of RyhB pairing with the SodA mRNA was properly increased (Figure 3B, solid lines). The individual effects of decreased RyhB production rate and increased pairing of RyhB and SodA mRNA were simulated for comparison (Figure 3B, dashed and dotted curves, respectively). As a result of lower RyhB production rate and more efficient complex formation between RyhB and SodA mRNA, the amplitude of the response decreased and the peak of the response occurred earlier. These effects are due to the improved ability of SodA mRNA to compete with the strong targets for RyhB binding [22]. Similar simulations with higher sRNA production rates and decreased pairing rates did not change the response curve.

The opposite effect was observed when the Fe-Fur concentration was suddenly increased (Figure 3C). In this case SodA mRNA levels decreased because Fe-Fur blocks only the production of SodA and RyhB mRNA, and it takes more than one cell generation to clear the existing RyhB sRNA molecules from the system.

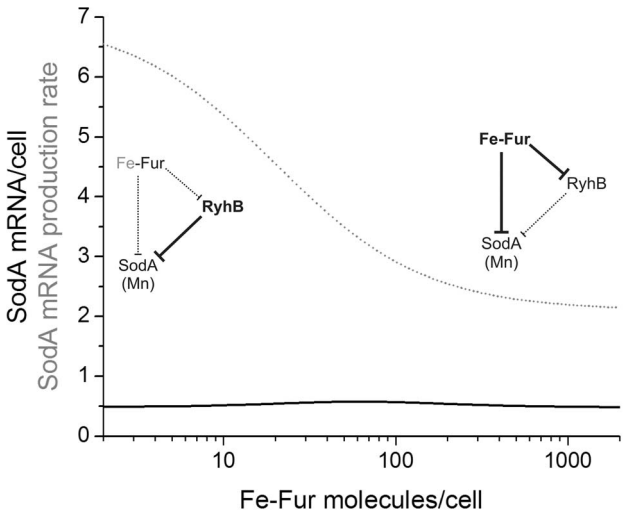

Figure 2. Steady state levels (solid black line) and production rate (dotted grey line) of SodA mRNA as a function of Fe-Fur level in the absence of superoxide stress. The functional interactions in the feed-forward loop at low and high Fe-Fur levels are shown in bold.
doi:10.1371/journal.pone.0091243.g002

Simulation of superoxide stress at low and high iron levels

Intracellular superoxide levels are sensed by the SoxR protein, which contains two [2Fe–2S] clusters. In its oxidized form, SoxR activates transcription of the SoxS protein, which regulates transcription of about 40 promoters. Induction of superoxide stress by paraquat results in about six-fold increase in sodA transcription [5]. Although sodA transcription is increased in Δ*fur* cells, similar fold activation was observed in wild type and Δ*fur* cells in the presence of paraquat [5]. Therefore in the model I assumed that SoxS and Fur act independently on the *sodA* promoter. Because SoxS in intrinsically unstable with an in vitro half-life of about 2 minutes [23], I simulated the effect of superoxide stress simply by increasing the maximal *sodA* transcription rate (Figure 4). I performed simulations at both low (1 nM) and high (2000 nM) Fe-Fur levels. At low Fe-Fur levels the FFL mediated system responded substantially faster than the constitutive system, both to the appearance and to the removal of superoxide stress (Figure 4 A and C). However, in the simulations at high Fe–Fur levels the response dynamics of SodA mRNA was indistinguishable in the FFL mediated and constitutive systems (Figure 4 B and D).

Discussion

In bacteria, small regulatory RNAs are often part of feed-forward motifs which contain both protein and RNA regulators (mixed FFLs) [24–26]. Unlike in pure transcriptional FFL motifs, where incoming regulatory signals must be integrated at the promoter of the target gene using a certain logic [20,27,28], in mixed motifs the actions of the protein and sRNA regulators on target production are spatially separated and independent of each other. The function of incoherent feed-forward loops in genetic regulation has been addressed both experimentally and theoretically. For example, incoherent FFLs were shown to accelerate response times [29], provide fold change detection [19], and generate non-monotonic input functions [30].

Regulatory effects of the mixed FFL

In this work I studied the function of a mixed FFL embedded into a small regulatory network that controls expression of cytoplasmic superoxide dismutases in *E. coli* (Figure 1). This system responds to two intracellular input signals, iron and superoxide concentrations. The system maintains SodA mRNA levels at a narrow concentration range at a wide range of iron

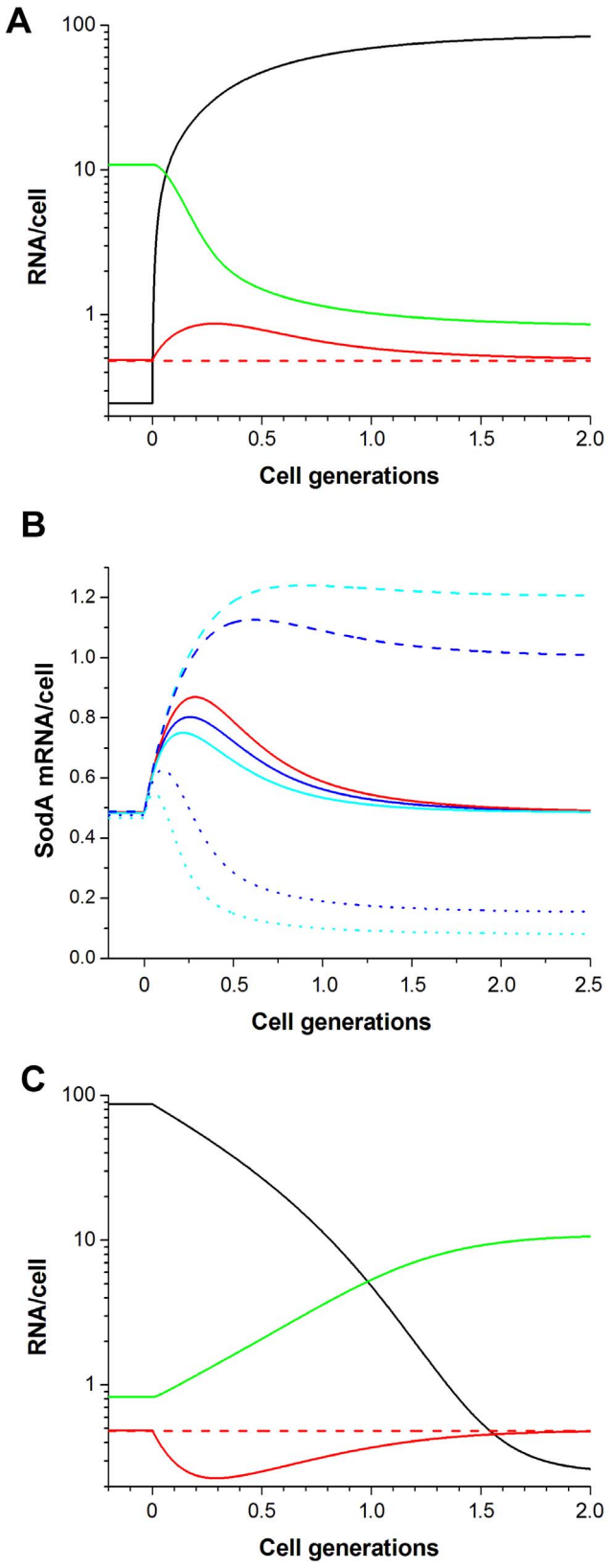

Figure 3. Simulations of transitions from high to low (A and B) and low to high (C) iron conditions in the absence of superoxide stress. The Fe-Fur concentration was changed at zero time from 2000 nM to 1 nM (A and B) or from 1 nM to 2000 nM (C). The solid black curves represent RyhB levels, while the solid red and green curves represent the levels of SodA and SodB mRNAs, respectively. The dashed red line represents the control system where SodA is produced constitutively. (B) Changes in the level of SodA mRNA were simulated using different sRNA production rates (α_S) and RyhB pairing rates (δ_A). The rate pairs used were chosen to obtain the same SodA mRNA levels at low and high iron conditions. The solid red curve represents simulations with the standard parameters ($\alpha_S = 280$/cell gen; $\delta_A = 0.0019$/min). The solid blue ($\alpha_S = 105$/cell gen; $\delta_A = 0.008$/min) and cyan ($\alpha_S = 70$/cell gen; $\delta_A = 0.016$/min) lines show simulations where the sRNA was produced at lower rates but formed a complex with the SodA mRNA at a higher rate. The dashed and dotted lines represent corresponding simulations when only the sRNA production rate was decreased or the complex formation rate was increased, respectively.
doi:10.1371/journal.pone.0091243.g003

concentrations, although the SodA mRNA turnover is higher at low iron levels (Figure 2). Similar to dominant negative autoregulatory systems [31], this FFL is mostly responsible for regulation of expression dynamics during transitions between different environmental conditions.

In the absence of superoxide, the system responds to changes in iron levels with similar pulse dynamics as was previously predicted for incoherent FFLs where the master regulator was an activator [19]. In the iron rich LB medium SodA and SodB transcript levels are similar [32]. However, iron levels greatly exceed manganese levels in *E. coli* grown in iron rich conditions [33], and a fraction of SodA proteins is inactive because being substituted by iron instead of manganese. When intracellular iron becomes scarce, the cell stops production of several non-essential iron using proteins, such as SodB, thus allowing essential proteins to utilize the available limited free iron pool [34].

The loss of SodB activity upon iron depletion is compensated on one hand by a decrease in the level of iron-substituted SodA, and on the other hand by a transiently increased SodA production (Figure 3A). Simulations of the transition from an iron-depleted to an iron rich environment predict the opposite effect (Figure 3C). In this case, SodA activity decreases because of the slower production and of the higher iron substitution rates as well.

Superimposed global controls

SodA expression is regulated by global regulators responding to intracellular iron and superoxide concentrations. The iron response system is acting through a mixed FFL, involving direct transcriptional and indirect translational regulation, while the superoxide response system acts directly at the transcriptional level (Figure 1). Because the FFL regulating SodA consists of global regulators which are used for regulation of many other genes, it does not generate an extra cost for the cell. Our simulations suggest that the major advantage of this FFL is that it can conditionally modulate the response time of a superimposed transcriptional control mechanism, allowing faster response of SodA when SodB function is limited. At low iron levels the superoxide stress response is predicted to be about three times faster compared to the control system, while at high iron levels the responses are identical (Figure 4). This effect is due to the mixed nature of the FFL, which allows differential regulation of SodA mRNA production and degradation rates by controlling transcription initiation (by Fe-Fur) and translation initiation/mRNA stability (by RyhB) separately. In the FFL regulated system the steady state SodA mRNA level is resulted from equilibrium of production, RyhB mediated degradation, natural degradation, and dilution. Compared to the FFL-regulated system, the constitutive system operates with a constant low SodA mRNA degradation rate, and therefore requires a smaller production rate to obtain the same steady state mRNA level. At low Fe-Fur levels, the FFL regulated system allows faster initial SodA mRNA

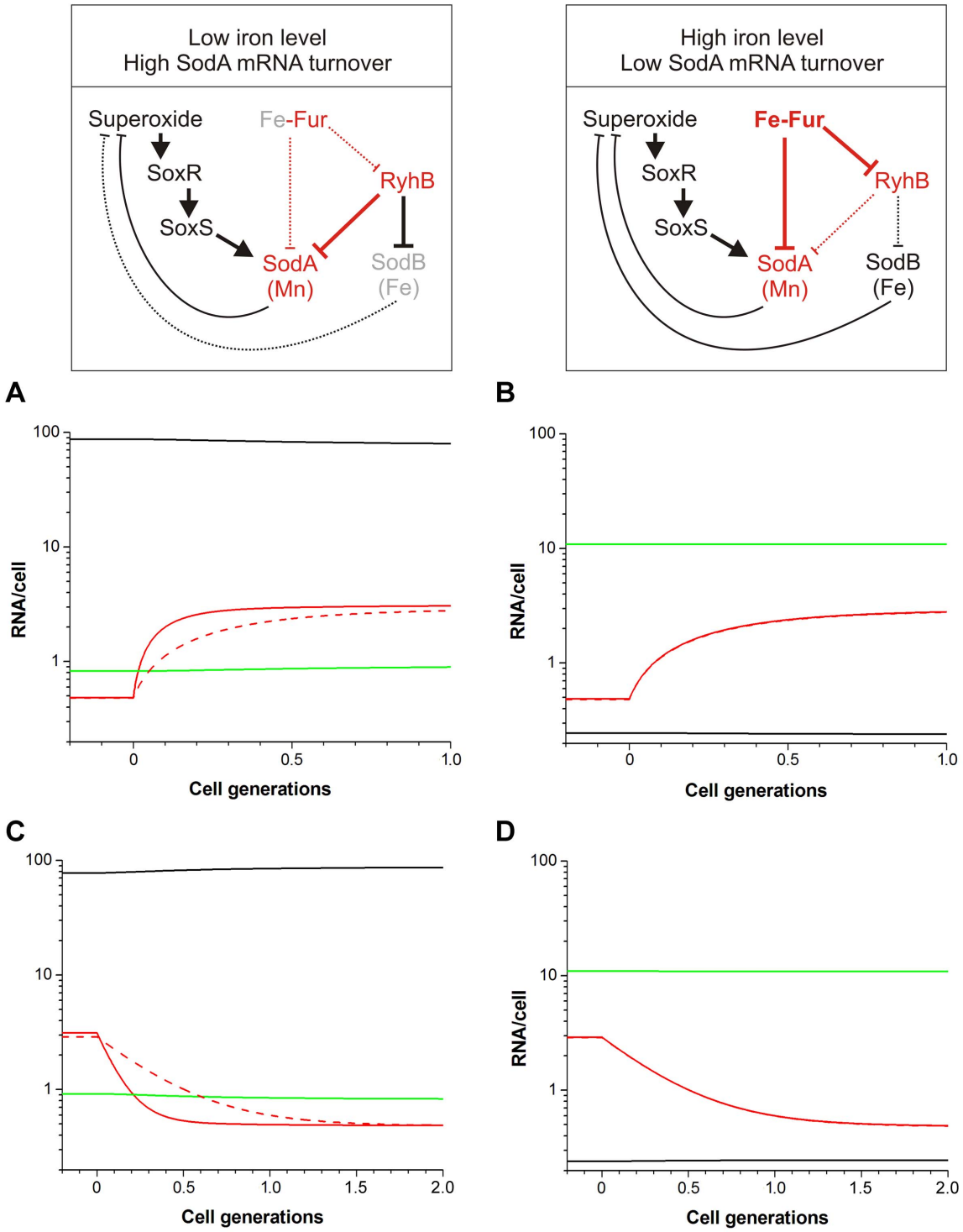

Figure 4. Simulations of changes in superoxide levels at low (left panels) and high (right panels) iron conditions. The dominant regulatory interactions are indicated on the top. At zero time the maximal transcription rate of SodA (α_A) was increased 6-fold (top panels) or decreased from this induced level to the uninduced level (bottom panels). The solid black curves represent RyhB levels, while the solid red and green curves represent the levels of SodA and SodB mRNAs, respectively. The dashed red line, which overlaps with the solid red curves in panels B and C, represents the control system where SodA is produced constitutively.
doi:10.1371/journal.pone.0091243.g004

production rate upon superoxide stress compared to the constitutive system, and reach a steady state quickly because of the increased RyhB mediated degradation, which is directly proportional to the level of SodA mRNA. The FFL also allows faster recovery from stress because of the active degradation of the existing SodA mRNAs.

In conclusion, the FFL allows faster superoxide stress response and better adaptation in iron restricted environments, such as

mammalian hosts. The same regulatory system is present in pathogenic strains (e.g. *E. coli* O104:H4, Shigella flexneri 2a str 301), suggesting that the fast response may help in inactivating superoxide molecules generated by the immune system.

Methods

The dynamical variables I keep track of in our model are the concentrations of RyhB (S), SodA mRNA (m_A), and SodB mRNA (m_B). Similar to previous models of sRNA regulation [22,34–37], I assume that: (i) the degradation of the sRNA-mRNA complex is faster than the dissociation of the same complex, so that the binding is effectively irreversible; (ii) both the sRNA and the mRNA are inactivated [38]; (iii) translation of the mRNA is not possible after the complex with the sRNA is formed. I also assume that 1 nM corresponds to one molecule per cell [39,40].

The deterministic differential equation that model RyhB dynamics is:

$$\frac{dS}{dt}=\frac{\frac{\alpha_S}{\tau_G}}{1+\frac{F}{K_D}}-\frac{S_{(t)}}{\tau_G}-\frac{S_{(t)}}{\tau_S}-\delta_A S_{(t)} m_{A(t)}-\delta_B S_{(t)} m_{B(t)} \quad \text{(I)}$$

The first term represents the production of RyhB, which is repressed by Fe-Fur (F). In this term, α_S is the maximal production rate of RyhB per cell generation time [41]. K_D ($=0.02$ μM) is the binding constant of Fe-Fur to its operator site [42]. In the second and third terms τ_S ($=30/\ln 2$ min) [38] and τ_G ($=40/\ln 2$ min) represents the passive degradation and dilution (by cell devision) of RyhB, respectively. The last two terms represent the active degradation of the RyhB-mRNA complexes by RNaseE [38]. SodA dynamics was modeled by the following equation

$$\frac{dm_A}{dt}=0.3\frac{\alpha_A}{\tau_G}+0.7\frac{\frac{\alpha_A}{\tau_G}}{1+\frac{F}{K_D}}-\frac{m_{A(t)}}{\tau_G}-\frac{m_{A(t)}}{\tau_A}-\delta_A S_{(t)} m_{A(t)} \quad \text{(II)}$$

Based on *sodA* promoter activities reported in wild type and Δ*fur* strains [8], I assume that that the *sodA* promoter has a basal activity even in the presence of Fe-Fur. The first term represents this basal activity, while the second term represents the Fe-Fur regulated activity. The effect of superoxide stress through the SoxR-SoxS system is not modeled explicitly; instead, it is simulated by increasing the maximal *sodA* promoter activity (α_A). The next two terms represent dilution and passive degradation ($\tau_A=11.8/\ln 2$ min) [32] of the SodA mRNA, while the last term represents the sRNA mediated degradation. The parameter for RyhB pairing with the SodA mRNA, δ_A, was chosen to be 0.0019/min to obtain similar SodA mRNA levels in the absence and in the presence of Fe-Fur [8].

The dynamics of SodB is modeled by the following equation:

$$\frac{dm_B}{dt}=\frac{\alpha_B}{\tau_G}-\frac{m_{B(t)}}{\tau_G}-\frac{m_{B(t)}}{\tau_B}-\delta_B S_{(t)} m_{B(t)} \quad \text{(III)}$$

The first term represents the production of SodB. The next two terms represent dilution and passive degradation ($\tau_B=8.8/\ln 2$ min) [32] of the SodB mRNA, while the last term represents the sRNA mediated degradation. The parameter for RyhB pairing with the SodB mRNA, δ_B, was chosen to be 0.014/min to reproduce the experimental observation that the SodB level in *Δfur* cells is 13% of the wild type level [43].

There are several other RyhB target mRNAs exist in the cell, which, similar to SodB, are not regulated directly by Fur. Therefore m_B represents all these mRNAs. The value for α_B (63 molecules per cell generation) was chosen based on the reported level of SodB mRNA (about 5 molecules/cell) [44] and on the estimate that SodB mRNA production constitutes about 40% of the production of strong targets [41].

The values of α_A, and α_S were chosen in such a way that $\alpha_A+\alpha_B=\alpha_S/4$ (representing the upper bound for α_S [41]), and SodA production was assumed to represent 10% of the production of all targets in the absence of superoxide stress ($\alpha_A=7$/cell generation). I compare the above natural system to a hypothetical one where SodA levels depend only on superoxide concentration and not on Fe-Fur or RyhB levels. In this case, equations I and III remain the same, and equation II becomes

$$\frac{dm_A}{dt}=\frac{\alpha_{AC}}{\tau_G}-\frac{m_{A(t)}}{\tau_G}-\frac{m_{A(t)}}{\tau_A}$$

where $\alpha_{AC}=\alpha_A/3.3$ to match the Fur-Fe regulated SodA level.

Acknowledgments

I thank Kim Sneppen and Namiko Mitarai for stimulating discussions and critical reading of the manuscript.

Author Contributions

Conceived and designed the experiments: SS. Performed the experiments: SS. Analyzed the data: SS. Wrote the paper: SS.

References

1. Diaz JM, Hansel CM, Voelker BM, Mendes CM, Andeer PF, et al. (2013) Widespread production of extracellular superoxide by heterotrophic bacteria. Science 340: 1223–1226.
2. El Bekay R, Alvarez M, Carballo M, Martin-Nieto J, Monteseirin J, et al. (2002) Activation of phagocytic cell NADPH oxidase by norfloxacin: a potential mechanism to explain its bactericidal action. J Leukoc Biol 71: 255–261.
3. Argaman L, Elgrably-Weiss M, Hershko T, Vogel J, Altuvia S (2012) RelA protein stimulates the activity of RyhB small RNA by acting on RNA-binding protein Hfq. Proc Natl Acad Sci U S A 109: 4621–4626.
4. Benov LT, Fridovich I (1994) Escherichia coli expresses a copper- and zinc-containing superoxide dismutase. J Biol Chem 269: 25310–25314.
5. Compan I, Touati D (1993) Interaction of six global transcription regulators in expression of manganese superoxide dismutase in Escherichia coli K-12. J Bacteriol 175: 1687–1696.
6. Fee JA (1991) Regulation of sod genes in Escherichia coli: relevance to superoxide dismutase function. Mol Microbiol 5: 2599–2610.
7. Niederhoffer EC, Naranjo CM, Bradley KL, Fee JA (1990) Control of Escherichia coli superoxide dismutase (sodA and sodB) genes by the ferric uptake regulation (fur) locus. J Bacteriol 172: 1930–1938.
8. Schrum LW, Hassan HM (1994) The effects of fur on the transcriptional and post-transcriptional regulation of MnSOD gene (sodA) in Escherichia coli. Arch Biochem Biophys 309: 288–292.
9. Mizuno K, Whittaker MM, Bachinger HP, Whittaker JW (2004) Calorimetric studies on the tight binding metal interactions of Escherichia coli manganese superoxide dismutase. J Biol Chem 279: 27339–27344.
10. Vance CK, Miller AF (1998) Spectroscopic comparisons of the pH dependencies of Fe-substituted (Mn)superoxide dismutase and Fe-superoxide dismutase. Biochemistry 37: 5518–5527.
11. Brown OR, Smyk-Randall E, Draczynska-Lusiak B, Fee JA (1995) Dihydroxy-acid dehydratase, a [4Fe-4S] cluster-containing enzyme in Escherichia coli: effects of intracellular superoxide dismutase on its inactivation by oxidant stress. Arch Biochem Biophys 319: 10–22.

12. Hopkin KA, Papazian MA, Steinman HM (1992) Functional differences between manganese and iron superoxide dismutases in Escherichia coli K-12. J Biol Chem 267: 24253–24258.
13. Pesce A, Capasso C, Battistoni A, Folcarelli S, Rotilio G, et al. (1997) Unique structural features of the monomeric Cu,Zn superoxide dismutase from Escherichia coli, revealed by X-ray crystallography. J Mol Biol 274: 408–420.
14. Benov L, Chang LY, Day B, Fridovich I (1995) Copper, zinc superoxide dismutase in Escherichia coli: periplasmic localization. Arch Biochem Biophys 319: 508–511.
15. Battistoni A, Donnarumma G, Greco R, Valenti P, Rotilio G (1998) Overexpression of a hydrogen peroxide-resistant periplasmic Cu,Zn superoxide dismutase protects Escherichia coli from macrophage killing. Biochem Biophys Res Commun 243: 804–807.
16. Gaudu P, Weiss B (1996) SoxR, a [2Fe–2S] transcription factor, is active only in its oxidized form. Proc Natl Acad Sci U S A 93: 10094–10098.
17. Masse E, Gottesman S (2002) A small RNA regulates the expression of genes involved in iron metabolism in Escherichia coli. Proc Natl Acad Sci U S A 99: 4620–4625.
18. Basu S, Mehreja R, Thiberge S, Chen MT, Weiss R (2004) Spatiotemporal control of gene expression with pulse-generating networks. Proc Natl Acad Sci U S A 101: 6355–6360.
19. Goentoro L, Shoval O, Kirschner MW, Alon U (2009) The incoherent feedforward loop can provide fold-change detection in gene regulation. Mol Cell 36: 894–899.
20. Mangan S, Alon U (2003) Structure and function of the feed-forward loop network motif. Proc Natl Acad Sci U S A 100: 11980–11985.
21. Takeda K, Shao D, Adler M, Charest PG, Loomis WF, et al. (2012) Incoherent feedforward control governs adaptation of activated ras in a eukaryotic chemotaxis pathway. Sci Signal 5: ra2.
22. Mitarai N, Andersson AM, Krishna S, Semsey S, Sneppen K (2007) Efficient degradation and expression prioritization with small RNAs. Phys Biol 4: 164–171.
23. Shah IM, Wolf RE, Jr. (2006) Sequence requirements for Lon-dependent degradation of the Escherichia coli transcription activator SoxS: identification of the SoxS residues critical to proteolysis and specific inhibition of in vitro degradation by a peptide comprised of the N-terminal 21 amino acid residues. J Mol Biol 357: 718–731.
24. Beisel CL, Storz G (2011) The base-pairing RNA spot 42 participates in a multioutput feedforward loop to help enact catabolite repression in Escherichia coli. Mol Cell 41: 286–297.
25. Shimoni Y, Friedlander G, Hetzroni G, Niv G, Altuvia S, et al. (2007) Regulation of gene expression by small non-coding RNAs: a quantitative view. Mol Syst Biol 3: 138.
26. Mank NN, Berghoff BA, Klug G (2013) A mixed incoherent feed-forward loop contributes to the regulation of bacterial photosynthesis genes. RNA Biol 10.
27. Hunziker A, Tuboly C, Horvath P, Krishna S, Semsey S (2010) Genetic flexibility of regulatory networks. Proc Natl Acad Sci U S A 107: 12998–13003.
28. Buchler NE, Gerland U, Hwa T (2003) On schemes of combinatorial transcription logic. Proc Natl Acad Sci U S A 100: 5136–5141.
29. Mangan S, Itzkovitz S, Zaslaver A, Alon U (2006) The incoherent feed-forward loop accelerates the response-time of the gal system of Escherichia coli. J Mol Biol 356: 1073–1081.
30. Kaplan S, Bren A, Dekel E, Alon U (2008) The incoherent feed-forward loop can generate non-monotonic input functions for genes. Mol Syst Biol 4: 203.
31. Semsey S, Krishna S, Erdossy J, Horvath P, Orosz L, et al. (2009) Dominant negative autoregulation limits steady-state repression levels in gene networks. J Bacteriol 191: 4487–4491.
32. Bernstein JA, Khodursky AB, Lin PH, Lin-Chao S, Cohen SN (2002) Global analysis of mRNA decay and abundance in Escherichia coli at single-gene resolution using two-color fluorescent DNA microarrays. Proc Natl Acad Sci U S A 99: 9697–9702.
33. Outten CE, O'Halloran TV (2001) Femtomolar sensitivity of metalloregulatory proteins controlling zinc homeostasis. Science 292: 2488–2492.
34. Semsey S, Andersson AM, Krishna S, Jensen MH, Masse E, et al. (2006) Genetic regulation of fluxes: iron homeostasis of Escherichia coli. Nucleic Acids Res 34: 4960–4967.
35. Lenz DH, Mok KC, Lilley BN, Kulkarni RV, Wingreen NS, et al. (2004) The small RNA chaperone Hfq and multiple small RNAs control quorum sensing in Vibrio harveyi and Vibrio cholerae. Cell 118: 69–82.
36. Levine E, Zhang Z, Kuhlman T, Hwa T (2007) Quantitative characteristics of gene regulation by small RNA. PLoS Biol 5: e229.
37. Sneppen K, Krishna S, Semsey S (2010) Simplified models of biological networks. Annu Rev Biophys 39: 43–59.
38. Masse E, Escorcia FE, Gottesman S (2003) Coupled degradation of a small regulatory RNA and its mRNA targets in Escherichia coli. Genes Dev 17: 2374–2383.
39. Halford SE, Marko JF (2004) How do site-specific DNA-binding proteins find their targets? Nucleic Acids Res 32: 3040–3052.
40. Semsey S, Jauffred L, Csiszovszki Z, Erdossy J, Steger V, et al. (2013) The effect of LacI autoregulation on the performance of the lactose utilization system in Escherichia coli. Nucleic Acids Res 41: 6381–6390.
41. Mitarai N, Benjamin JA, Krishna S, Semsey S, Csiszovszki Z, et al. (2009) Dynamic features of gene expression control by small regulatory RNAs. Proc Natl Acad Sci U S A 106: 10655–10659.
42. Mills SA, Marletta MA (2005) Metal binding characteristics and role of iron oxidation in the ferric uptake regulator from Escherichia coli. Biochemistry 44: 13553–13559.
43. Dubrac S, Touati D (2000) Fur positive regulation of iron superoxide dismutase in Escherichia coli: functional analysis of the sodB promoter. J Bacteriol 182: 3802–3808.
44. Arbel-Goren R, Tal A, Friedlander T, Meshner S, Costantino N, et al. (2013) Effects of post-transcriptional regulation on phenotypic noise in Escherichia coli. Nucleic Acids Res 41: 4825–4834.